Digital phase conjugation of second harmonic radiation emitted by nanoparticles in turbid media

Chia-Lung Hsieh,[1,2*] Ye Pu,[1] Rachel Grange,[1] and Demetri Psaltis[1]

[1]*School of Engineering, EPFL, Station 17, 1015 Lausanne, Switzerland*
[2]*Department of Electrical Engineering, California Institute of Technology, 1200 East California Boulevard, MC 136-93, Pasadena, California 91125, USA*
**chia-lung.hsieh@epfl.ch*

Abstract: We demonstrate focusing coherent light on a nanoparticle through turbid media based on digital optical phase conjugation of second harmonic generation (SHG) field from the nanoparticle. A SHG active nanoparticle inside a turbid medium was excited at the fundamental frequency and emitted SHG field as a point source. The SHG emission was scattered by the turbid medium, and the scattered field was recorded by off-axis digital holography. A phase-conjugated beam was then generated by using a phase-only spatial light modulator and sent back through the turbid medium, which formed a nearly ideal focus on the nanoparticle.

OCIS codes: (070.5040) Phase conjugation; (090.1995) Digital holography; (110.0113) Imaging through turbid media; (160.4236) Nanomaterials; (160.4330) Nonlinear optical materials; (290.7050) Turbid media.

References and links

1. F. Helmchen, and W. Denk, "Deep tissue two-photon microscopy," Nat. Methods **2**(12), 932–940 (2005).
2. E. N. Leith, and J. Upatniek, "Holographic imagery through diffusing media," J. Opt. Soc. Am. **56**, 523 (1966).
3. H. Kogelnik, and K. S. Pennington, "Holographic imaging through a random medium," J. Opt. Soc. Am. **58**, 273–274 (1968).
4. M. Rueckel, J. A. Mack-Bucher, and W. Denk, "Adaptive wavefront correction in two-photon microscopy using coherence-gated wavefront sensing," Proc. Natl. Acad. Sci. U.S.A. **103**(46), 17137–17142 (2006).
5. I. M. Vellekoop, and A. P. Mosk, "Focusing coherent light through opaque strongly scattering media," Opt. Lett. **32**(16), 2309–2311 (2007).
6. I. M. Vellekoop, and A. P. Mosk, "Universal optimal transmission of light through disordered materials," Phys. Rev. Lett. **101**(12), 120601(2008).
7. Z. Yaqoob, D. Psaltis, M. S. Feld, and C. Yang, "Optical phase conjugation for turbidity suppression in biological samples," Nat. Photonics **2**(2), 110–115 (2008).
8. M. Cui, E. J. McDowell, and C. H. Yang, "An in vivo study of turbidity suppression by optical phase conjugation (TSOPC) on rabbit ear," Opt. Express **18**(1), 25–30 (2010).
9. M. Cui, and C. H. Yang, "Implementation of a digital optical phase conjugation system and its application to study the robustness of turbidity suppression by phase conjugation," Opt. Express **18**(4), 3444–3455 (2010).
10. N. Ji, D. E. Milkie, and E. Betzig, "Adaptive optics via pupil segmentation for high-resolution imaging in biological tissues," Nat. Methods **7**(2), 141–147 (2010).
11. I. M. Vellekoop, A. Lagendijk, and A. P. Mosk, "Exploiting disorder for perfect focusing," Nat. Photonics Advance online publication, DOI: 10.1038/NPHOTON.2010.3 (2010).
12. J. C. Johnson, H. Q. Yan, R. D. Schaller, P. B. Petersen, P. D. Yang, and R. J. Saykally, "Near-field imaging of nonlinear optical mixing in single zinc oxide nanowires," Nano Lett. **2**(4), 279–283 (2002).
13. S. Brasselet, V. Le Floc'h, F. Treussart, J. F. Roch, J. Zyss, E. Botzung-Appert, and A. Ibanez, "In situ diagnostics of the crystalline nature of single organic nanocrystals by nonlinear microscopy," Phys. Rev. Lett. **92**(20), 207401 (2004).
14. E. Delahaye, N. Tancrez, T. Yi, I. Ledoux, J. Zyss, S. Brasselet, and R. Clement, "Second harmonic generation from individual hybrid MnPS3-based nanoparticles investigated by nonlinear microscopy," Chem. Phys. Lett. **429**(4-6), 533–537 (2006).
15. L. L. Xuan, S. Brasselet, F. Treussart, J.-F. Roch, F. Marquier, D. Chauvat, S. Perruchas, C. Tard, and T. Gacoin, "Balanced homodyne detection of second-harmonic generation from isolated subwavelength emitters," Appl. Phys. Lett. **89**(12), 121118 (2006).

#127173 - $15.00 USD Received 19 Apr 2010; revised 19 May 2010; accepted 23 May 2010; published 25 May 2010

16. L. Bonacina, Y. Mugnier, F. Courvoisier, R. Le Dantec, J. Extermann, Y. Lambert, V. Boutou, C. Galez, and J. P. Wolf, "Polar Fe(IO3)(3) nanocrystals as local probes for nonlinear microscopy," Appl. Phys. B **87**(3), 399–403 (2007).
17. Y. Nakayama, P. J. Pauzauskie, A. Radenovic, R. M. Onorato, R. J. Saykally, J. Liphardt, and P. D. Yang, "Tunable nanowire nonlinear optical probe," Nature **447**(7148), 1098–1101 (2007).
18. N. Sandeau, L. Le Xuan, D. Chauvat, C. Zhou, J. F. Roch, and S. Brasselet, "Defocused imaging of second harmonic generation from a single nanocrystal," Opt. Express **15**(24), 16051–16060 (2007).
19. A. V. Kachynski, A. N. Kuzmin, M. Nyk, I. Roy, and P. N. Prasad, "Zinc oxide nanocrystals for nonresonant nonlinear optical microscopy in biology and medicine," J. Phys. Chem. C **112**(29), 10721–10724 (2008).
20. X. L. Le, C. Zhou, A. Slablab, D. Chauvat, C. Tard, S. Perruchas, T. Gacoin, P. Villeval, and J. F. Roch, "Photostable second-harmonic generation from a single KTiOPO4 nanocrystal for nonlinear microscopy," Small **4**(9), 1332–1336 (2008).
21. Y. Pu, M. Centurion, and D. Psaltis, "Harmonic holography: a new holographic principle," Appl. Opt. **47**(4), A103–A110 (2008).
22. J. Extermann, L. Bonacina, E. Cuña, C. Kasparian, Y. Mugnier, T. Feurer, and J. P. Wolf, "Nanodoublers as deep imaging markers for multi-photon microscopy," Opt. Express **17**(17), 15342–15349 (2009).
23. C. L. Hsieh, R. Grange, Y. Pu, and D. Psaltis, "Three-dimensional harmonic holographic microcopy using nanoparticles as probes for cell imaging," Opt. Express **17**(4), 2880–2891 (2009).
24. T. R. Kuo, C. L. Wu, C. T. Hsu, W. Lo, S. J. Chiang, S. J. Lin, C. Y. Dong, and C. C. Chen, "Chemical enhancer induced changes in the mechanisms of transdermal delivery of zinc oxide nanoparticles," Biomaterials **30**(16), 3002–3008 (2009).
25. E. M. Rodríguez, A. Speghini, F. Piccinelli, L. Nodari, M. Bettinelli, D. Jaque, and J. G. Sole, "Multicolour second harmonic generation by strontium barium niobate nanoparticles," J. Phys. D Appl. Phys. **42**(10), 102003 (2009).
26. E. V. Rodriguez, C. B. Araújo, A. M. Brito-Silva, V. I. Ivanenko, and A. A. Lipovskii, "Hyper-Rayleigh scattering from BaTiO3 and PbTiO3 nanocrystals," Chem. Phys. Lett. **467**(4-6), 335–338 (2009).
27. P. Wnuk, L. L. Xuan, A. Slablab, C. Tard, S. Perruchas, T. Gacoin, J.-F. Roch, D. Chauvat, and C. Radzewicz, "Coherent nonlinear emission from a single KTP nanoparticle with broadband femtosecond pulses," Opt. Express **17**(6), 4652–4658 (2009).
28. M. Zielinski, D. Oron, D. Chauvat, and J. Zyss, "Second-harmonic generation from a single core/shell quantum dot," Small **5**(24), 2835–2840 (2009).
29. C. L. Hsieh, R. Grange, Y. Pu, and D. Psaltis, "Bioconjugation of barium titanate nanocrystals with immunoglobulin G antibody for second harmonic radiation imaging probes," Biomaterials **31**(8), 2272–2277 (2010).
30. E. Shaffer, N. Pavillon, J. Kühn, and C. Depeursinge, "Digital holographic microscopy investigation of second harmonic generated at a glass/air interface," Opt. Lett. **34**(16), 2450–2452 (2009).
31. O. Masihzadeh, P. Schlup, and R. A. Bartels, "Label-free second harmonic generation holographic microscopy of biological specimens," Opt. Express **18**(10), 9840–9851 (2010).
32. S. L. Jacques, "Time-resolved reflectance spectroscopy in turbid tissues," IEEE Trans. Biomed. Eng. **36**(12), 1155–1161 (1989).
33. J. Extermann, L. Bonacina, F. Courvoisier, D. Kiselev, Y. Mugnier, R. Le Dantec, C. Galez, and J.-P. Wolf,"Nano-FROG: Frequency resolved optical gating by a nanometric object," Opt. Express **16**(14), 10405–10411 (2008).

1. Introduction

Focusing light through turbid media is a highly sought after capability for imaging applications but its implementation remains challenging. The inhomogeneous optical properties in the sample perturb the wave-front of the focusing light and seriously degrade the quality of the focus. For most biomedical imaging applications, especially in vivo tissue imaging, the strong scattering of the biological specimen limits the penetration depth [1]. Adaptive optics aims to suppress the scattering effect by measuring and then correcting for the inhomogeneities [2–11]. The suppression of scattering effects has been demonstrated by tailoring the wave-front of the incident light properly [2–11]. The ability to focus through a turbid medium increases the imaging depth and resolution in a fluorescence imaging system. Furthermore, it offers the opportunity to minimize the light dosage for photothermal therapy: instead of shining a strong beam being diffused in the scattering sample, one can use a shaped wave-front to deliver the optical energy to the target with pin-point precision and trigger the therapeutic event.

One of the methods to tailor the wave-front for optimal focusing is based on a feedback loop between the active wave-front modulator and the detection of the quality of the focus

#127173 - $15.00 USD Received 19 Apr 2010; revised 19 May 2010; accepted 23 May 2010; published 25 May 2010

[5,6,10,11]. Through optimization algorithms, one can find the optimal wave-front that cancels out the scattering and forms the focus on the sample. For microscopy, the detection of the quality of the focus is usually reported by the fluorescent probe at the focus inside the sample. As a result, the wave-front is tailored to form an optimal focus on the fluorescent probe.

Another method to find the optimal wave-front for focusing is based on optical phase conjugation [2,3,7–9]. In optical phase conjugation, a coherent point source is placed inside the turbid sample and the scattered field is recorded from the outside of the sample by holography. The phase-conjugated scattered field is then generated from the recorded hologram and sent back to the sample. The turbid medium will undo the initial scattering and a focus will form at the position where the coherent light source is initially placed. Focusing through a biological tissue by phase conjugation was demonstrated with a photorefractive crystal, which accommodates the holographic recording and the generation of the phase-conjugated scattered field [7,8]. Recently it has been reported that the optical phase conjugation can be done all-digitally [9]: the scattered field is recorded by digital holography and the phase-conjugated beam is generated by using a spatial light modulator (SLM). Digital optical phase conjugation has the potential to be a fast and efficient adaptive optics technique. The phase-conjugated beam is adapted to the recorded scattered field without iterative optimization algorithm.

If we wish to focus a light beam inside a turbid medium using optical phase conjugation, the main challenge is to have a coherent point source inside the turbid sample. Such a coherent source is very difficult to obtain by using linear optical approaches due to the strong background linear scattering of the turbid medium. In this paper, we demonstrate a nonlinear optical approach to such focusing using digital phase conjugation and second harmonic generation (SHG) active nanomaterials as the local coherent sources. Non-centrosymmetric nanomaterials have been demonstrated as efficient SHG sub-wavelength sources [12–29]. Only materials with crystalline structures lacking a center of symmetry are capable of efficient SHG. As a result, when imaging at the SHG frequency, these nanomaterials provide a strong contrast in a generally unstructured or isotropic turbid environment. We refer to these SHG-active nanocrystals as "Second Harmonic Radiation IMaging Probes (SHRIMPs)." When a SHRIMP inside a turbid sample is excited at the fundamental frequency, it emits coherent SHG signal at the doubled frequency like a point source. Therefore, a coherent point source at the SHG frequency for optical phase conjugation can be obtained without any prior knowledge of the turbid sample. The SHG scattered field from the SHRIMP is recorded by off-axis digital holography. The phase-conjugated SHG field is calculated and generated by using a phase-only SLM. The phase-conjugated field is then sent back to the sample, and it forms a nearly ideal focus spot on the SHRIMP inside a turbid sample.

2. Sample preparation and experimental setup

We used 300-nm (in diameter) barium titanate ($BaTiO_3$) nanocrystals as the SHRIMPs. The crystal structure of the $BaTiO_3$ nanocrystals is tetragonal which is non-centrosymmetric and allows for efficient SHG without further treatment. The $BaTiO_3$ nanocrystals were deposited on a microscope cover slip (~145 μm in thickness). The turbid medium is composed of two layers of Parafilm M laboratory film (~130 μm in thickness each) attached on a cover slip by two layers of double-sided tape (~80 μm in thickness each, Scotch, 3M). Assuming the absorption of the turbid medium at 400 nm wavelength is negligible, we measured the quantity of $\mu_s l$ (μ_s, effective scattering coefficient, l, thickness of the sample) of the turbid medium at 400 nm wavelength by measuring the transmitted ballistic light. Experimentally, a collimated 1-mm-diameter pulse laser beam centered at 400 nm wavelength was obtained by frequency doubling a Ti:sapphire oscillator (150 fs laser pulses at 80 MHz centered at 800 nm) with a β-barium borate (BBO) crystal. The laser beam illuminated the scattering medium, and the transmitted light was estimated by measuring the portion of light transmitted through

#127173 - $15.00 USD Received 19 Apr 2010; revised 19 May 2010; accepted 23 May 2010; published 25 May 2010

a 1-mm-diameter iris placed 3 meters away from the turbid medium. The $\mu_s l$ of the turbid medium was measured to be ~8.5. With the effective thickness of the scattering medium as ~420 μm (two layers of the Parafilm and two layers of the double-sided tape), the effective scattering coefficient is estimated to be ~200 cm^{-1}. For the demonstration of the concept, we placed the SHRIMPs and scattering medium on two independent sample holders which are 1 mm apart from each other as shown in Fig. 1.

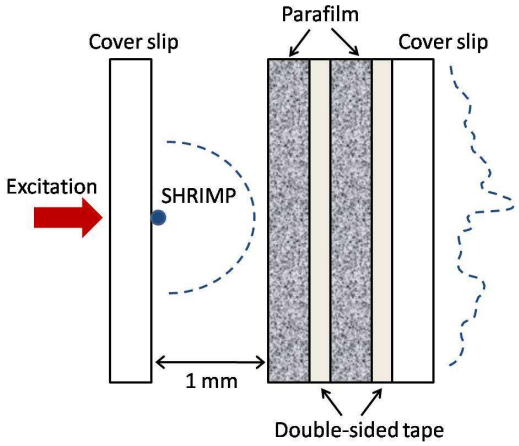

Fig. 1. Schematic diagram of the sample structure.

The experimental setup is shown in Fig. 2. The excitation light source is a Ti:sapphire oscillator generating 150 fs laser pulses at 80 MHz centered at 800 nm. The excitation is focused by a 10x microscope objective (NA 0.25, OBJ1 in Fig. 2) onto the SHRIMP. The average excitation power is approximately 50 mW. The SHG signal from the SHRIMP emits in both forward and backward directions. The epi-SHG signal is collected by the same microscope objective (OBJ1), reflected by a dichroic mirror, and then imaged on a charge-coupled device (CCD) camera (Scion, CFW-1312M, CCD1 in Fig. 2) with a lens of 20-cm focal length (L1).

The forward SHG signal is scattered by the turbid medium after propagating in air by 1 mm. The scattered SHG field is recorded by a harmonic holographic (H^2) microscope [21,23,30,31]. The H^2 microscope can be understood as a 4F imaging system followed by a holographic recording system. The scattered SHG field from the SHRIMP is collected and optically magnified by a 4F system consisting of a 10x microscope objective (NA 0.25, OBJ2 in Fig. 2) and a lens of 20 cm focal length (L2). The detector of the H^2 microscope is an electron multiplying charge coupled device (EMCCD, Andor iXonEM + 885) camera (CCD2 in Fig. 2). We put the CCD2 away from the 4F imaging plane so that the scattered field could propagate and fill the detection area of EMCCD. The hologram recording distance, i.e. the distance between the SHG image formed by the 4F system and the EMCCD, is 20 cm. A plane wave at the SHG frequency generated by a separate BBO crystal served as the reference beam. By overlapping the scattered field and reference beam both spatially and temporally on the CCD2, we record an off-axis digital hologram of the scattered SHG field. The angle between the signal and reference arms is ~1 degree. The complex scattered SHG field is then extracted from the recorded off-axis digital hologram.

#127173 - $15.00 USD Received 19 Apr 2010; revised 19 May 2010; accepted 23 May 2010; published 25 May 2010

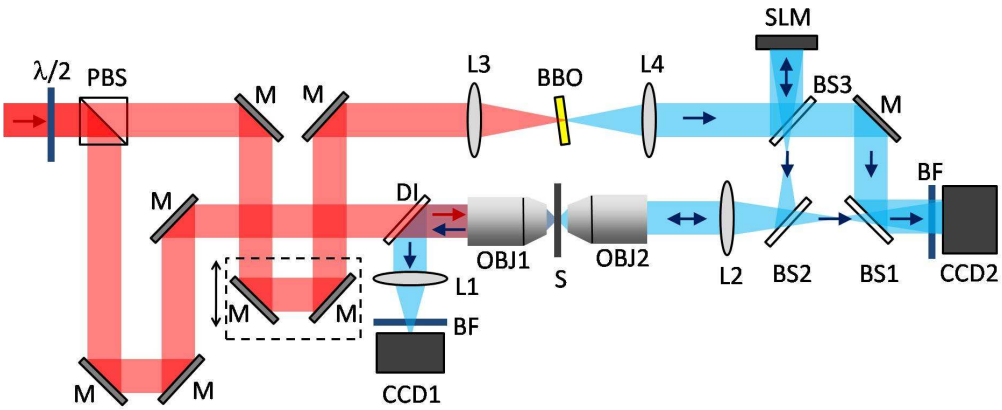

Fig. 2. Digital phase conjugation experimental setup. λ/2, half wave plate; PBS, polarization beam splitter; M, mirror; DI, dichroic mirror; L1 – L4, lens; OBJ1 and OBJ2, microscope objectives; S, sample; BS1 – BS3, non-polarizing beam splitters; BF, band-pass filter centered at 400 nm. The laser power for SHRIMP excitation and phase conjugation can be controlled by the λ/2 and the PBS. A translation stage was used to overlap the signal and the reference pulses temporally for the H^2 microscopy. Band-pass filters are placed in front of the CCD cameras to remove the excitation from the SHG signal.

We digitally conjugate the phase of the measured scattered field and project it on to a phase-only reflective SLM (PLUTO-VIS, HOLOEYE). The pixel size of the SLM is 8 x 8 μm^2, which matches with the pixel size of the CCD2. A plane wave at the SHG frequency is incident on the SLM and picks up the conjugated phase pattern after the reflection. The phase-conjugated beam is delivered back to the turbid medium through the 4F system. When the optical system is well aligned (i.e. the CCD2 and the SLM are aligned pixel by pixel), the turbid medium will undo the scattering and the phase-conjugated beam is expected to form a focus on the SHRIMP. We evaluate the phase-conjugated focus with the imaging system placed in the epi-geometry (i.e. OBJ1, L1 and CCD1).

3. Results and discussion

We started the measurement without scattering media. An isolated SHRIMP was excited and the epi-SHG image was observed on the CCD1, which is shown in Fig. 3 (a). The full-width at half-maximum (FWHM) of the spot is measured to be 1.95 μm which is the diffraction limit. The SHRIMP acts as a point source at SHG frequency and the emitted SHG field is similar to a spherical wave in the far field. Therefore, the phase of the SHG field recorded by the H^2 microscope is a spherical wave-front. The conjugation of the measured phase is a Fresnel zone plate as shown in Fig. 3 (b). The Fresnel zone plate was projected on to the SLM, and the phase-conjugated beam formed a focus on the SHRIMP after passing through the 4F system. We blocked the excitation and used the epi-imaging system (i.e. OBJ1, L1 and CCD1) to monitor the phase-conjugated focus. When the optical system is well aligned, the focus is exactly located on the SHRIMP. The presence of the SHRIMP at the phase-conjugated focus disturbs the phase-conjugated focus due to the scattering of the SHRIMP. Therefore, we removed the SHRIMP from the focus to evaluate the quality of the phase conjugation. The phase-conjugated focus is shown in Fig. 3 (c). The FWHM of the phase-conjugated focus is 1.95 μm, showing a good quality of the phase conjugation through a clear medium.

#127173 - $15.00 USD Received 19 Apr 2010; revised 19 May 2010; accepted 23 May 2010; published 25 May 2010

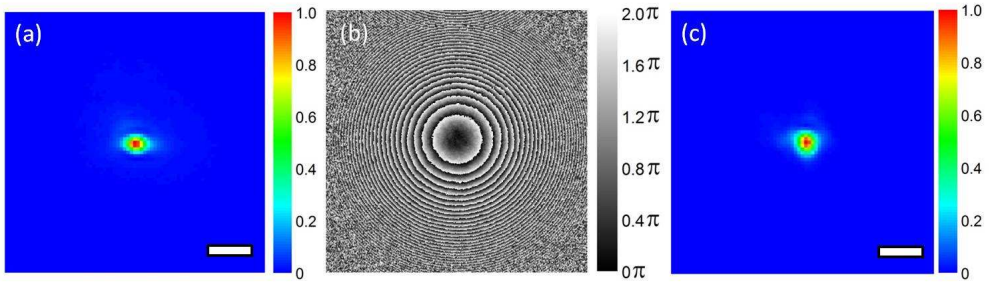

Fig. 3. Digital phase conjugation through a clear medium. (a) The epi-SHG image of the SHRIMP under excitation. (b) The conjugated phase pattern of the recorded SHG field emitted from the SHRIMP, showing a Fresnel zone plate. (c) The phase-conjugated focus formed at the sample by using the Fresnel zone plate shown in (b). The FWHM of the bright spots in (a) and (c) is 1.95 μm. The scale bars in the figures are 5 μm.

We then placed the turbid medium 1 mm away from the sample of SHRIMPs as shown in Fig. 1 and repeated the measurement. The SHG field from the SHRIMP under excitation was scattered and recorded by the H^2 microscope. The acquisition time of the digital hologram is approximately 1 second. The conjugation of the measured phase is shown in Fig. 4 (a). The random phase information implies the phase of the SHG field has been severely disturbed by the scattering media. When the phase pattern in Fig. 4 (a) was projected on the SLM, the phase-conjugated beam was able to form a focus at the position where the SHRIMP was located as shown in Fig. 4 (b). The FWHM of the conjugated focus in Fig. 4 (b) is 2.3 μm, which is close to the diffraction limit of the system. When we used the Fresnel zone plate pattern (as shown in Fig. 3 (b)) on the SLM, no focus could be formed through the turbid medium due to the scattering. A speckle pattern was observed as shown in Fig. 4 (c). Comparing Fig. 4 (b) and (c), it is clear that much more optical power is delivered to the focus spot when the phase conjugation is performed with the measured phase pattern. The ratio between the total power within the phase-conjugated bright spot (within the FWHM area) and the average power of the speckle pattern within the same size of area is measured to be 30. In Fig. 5, we plot and compare the intensity profiles of the diffraction limited focus (as shown in Fig. 3 (c)) and the phase-conjugated focus through the turbid medium (as shown in Fig. 4 (b)). Nearly ideal focus was obtained by the digital phase conjugation through the turbid medium.

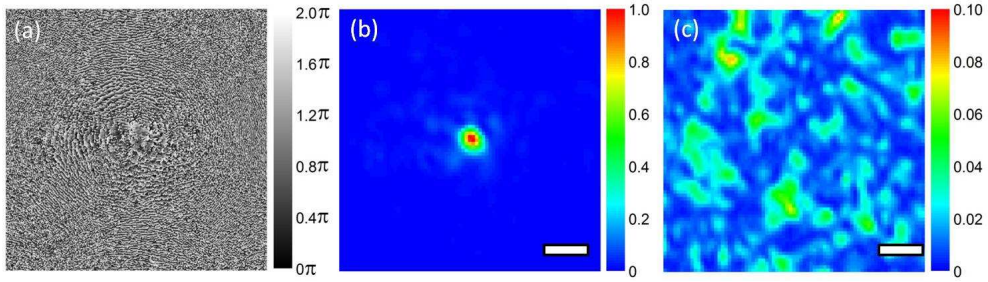

Fig. 4. Digital phase conjugation through a turbid medium. (a) The conjugated phase pattern of the scattered SHG field. (b) The normalized intensity image of the phase-conjugated focus through a turbid medium by using the phase pattern shown in (a). The FWHM of the spot is 2.3 μm. (c) The normalized intensity image of the distorted focus when using the Fresnel zone plate (as shown in Fig. 3 (b)) as the phase pattern. No focus is observed. Note that (b) and (c) are measured with the same power of the phase-conjugated beams and they are normalized by the same factor in the image processing. The scale bars in the figures are 5 μm.

#127173 - $15.00 USD Received 19 Apr 2010; revised 19 May 2010; accepted 23 May 2010; published 25 May 2010

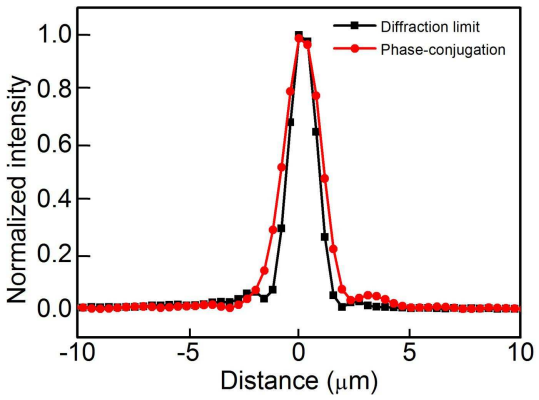

Fig. 5. Comparison of the measured diffraction limited focus and the phase-conjugated focus. Black: the normalized intensity profile of the diffraction limited focus; red: the normalized intensity profile of the phase-conjugated focus. The FWHMs of the diffraction limited focus and the phase-conjugated focus are 1.95 μm and 2.3 μm respectively.

The phase-conjugated focusing we observed was remarkable considering that we captured only a portion of the scattered field. The SHG signal emitted from the SHRIMP under excitation is a femtosecond laser pulse. When it is incident on the turbid medium, the pulse will spread temporally into a ballistic component and a diffuse component due to the scattering [32]. In our digital holographic recording, the coherence length of the reference beam is ~150 fs (determined by the laser pulse width) which is only able to capture part of the diffused scattered field. We adjusted the time of the reference pulse arriving at the CCD camera so that the strongest contrast of the hologram was observed. The holography faithfully recorded part of the scattered field within the coherence length of the reference pulse. In our phase conjugation setup, a plane wave of ~150 fs pulse width was used to carry the conjugated phase pattern. As a result, it can be understood that the phase conjugation was performed only for the holographic-recorded portion of the scattered field. The phase-conjugated focusing can be improved if the temporal diffused light is considered. It has been reported that the local complex field with temporal information can be measured by using SHG-active nanoparticles [33]. We expect an optimal spatio-temporal focusing can be achieved by combining optical phase conjugation and proper pulse shaping.

It is worth noting the role of polarization in our experiment. The laser at the fundamental frequency was divided into s- and p-polarizations by a polarization beam splitter (PBS in Fig. 2). The s-polarization was used to excite the SHRIMP. The p-polarization was frequency doubled by a BBO crystal through type I phase matching, so the polarization of the reference beam and the phase-conjugated beam at the SHG frequency were s-polarized. The SHRIMP under s-polarized excitation emits the SHG signal in all polarizations through the second-order nonlinear susceptibility tensor [23]. The SHRIMP signal is then being scattered by the turbid medium, which further depolarizes the signal. When using an s-polarized reference beam, we only capture the s-polarized component of the scattered SHG field of the SHRIMP. The information contained in the p-polarized scattered field is discarded. Therefore, the digital phase conjugation is only performed for s-polarized scattered field. We expect a better quality of the phase-conjugated focus if both of the polarizations are considered.

It is also critical to consider the resolution of our optical system compared to the size of the speckles in the scattered field. When the turbid medium is highly scattering, the scattered field at the output surface of the turbid media can have a speckle size approaching to the diffraction limited of light (~0.24 μm FWHM at 400 nm wavelength). This is because the turbid medium scatters light in all the directions randomly so that a broad angular distribution of the scattered light can be possibly formed, which leads to a small speckle size. In our experiment, the resolution of the optical system is ~0.98 μm, limited by the NA 0.25

#127173 - $15.00 USD Received 19 Apr 2010; revised 19 May 2010; accepted 23 May 2010; published 25 May 2010

microscope objective. The scattered field of higher spatial frequency would not be captured in the hologram, and therefore, not be considered in the phase conjugation. Besides, the scattered field is recorded by off-axis holography which inevitably degrades the resolution of the optical system. To minimize this effect, we experimentally remove the non-interferometric part (i.e. the signal and reference) from the digital hologram by subtracting a background of the two pulses not being temporally overlapped. As a result, the spatial resolution is controlled to be decreased by a factor of 2 in only one transversal direction. The resolution of the optical system can be increased by using a higher NA microscope objective, and thus a tighter phase-conjugated focus is achievable.

4. Conclusion

We demonstrated focusing coherent light on a nanoparticle through a turbid medium ($\mu_s l$ ~8.5) based on the digital phase conjugation of the SHG signal emitted from the nanoparticle. Non-centrosymmetric nanoparticles act as coherent point sources at SHG frequency under excitation which provide great contrast in a turbid medium for optical phase conjugation. We observed a nearly ideal focus on the nanoparticle through digital phase conjugation. 30 times more optical power was successfully delivered to the diffraction limit area centered at the nanoparticle in our experiment. Our work enables concentrating optical energy on the nanoparticles inside a turbid medium. While 300 nm $BaTiO_3$ particles were used in our demonstration, our approach can be easily extended to smaller SHG-active nanoparticles. We expect in the future to be able to use smaller particles by improving the sensitivity of the detector and the SHG efficiency of the nanoparticles [28]. Combining the phase conjugation technique with the functionalized SHRIMPs [29], one can specifically label the targets of interest inside the turbid medium with the SHRIMPs and then deliver the optical power efficiently to the desired locations.

Acknowledgements

The authors thank Dr. Paul Bowen at EPFL for providing the $BaTiO_3$ nanocrystals. This project is supported by the National Center of Competence in Research (NCCR), Quantum Photonics.

#127173 - $15.00 USD Received 19 Apr 2010; revised 19 May 2010; accepted 23 May 2010; published 25 May 2010